

An Integrated Optical CO₂ Sensor

Phase 0 Final Report:

Design and Fabrication of Critical Elements

DATE: DECEMBER 1994

Handwritten notes:
11-11-94
OCT.
5-5-94
1-

ATTENTION: Mr. John Hines
Manager, Sensors 2000
NASA Ames Research Center
Moffett Field, MS 213-2
Mountain View, CA 94035

PRINCIPAL INVESTIGATOR:

Michael C. Murphy, Ph.D.
2508 CEBA
Mechanical Engineering Department
Louisiana State University
Baton Rouge, LA 70803
Phone: (504) 388-5921
FAX: (504) 388-5990
e-mail: memcm@lsuvax.lsu.edu

CO-INVESTIGATORS:

Kevin W. Kelly, Ph.D.
B.Q. Li, Ph.D.
En Ma, Ph.D.
Wanjun Wang, Ph.D.
2508 CEBA
Mechanical Engineering Department
Louisiana State University
Baton Rouge, LA 70803

Yuli Vladimirovsky, Ph.D.
Olga Vladimirovsky
Center for Advanced Microstructures
and Devices
Louisiana State University
3990 W. Lakeshore Drive
Baton Rouge, LA 70803

(NASA-CR-198792) AN INTEGRATED OPTICAL CO₂ SENSOR. PHASE 0: DESIGN AND FABRICATION OF CRITICAL ELEMENTS Final Report (Louisiana State Univ.) 18 p

N95-29366

Unclass

G3/74 0055112

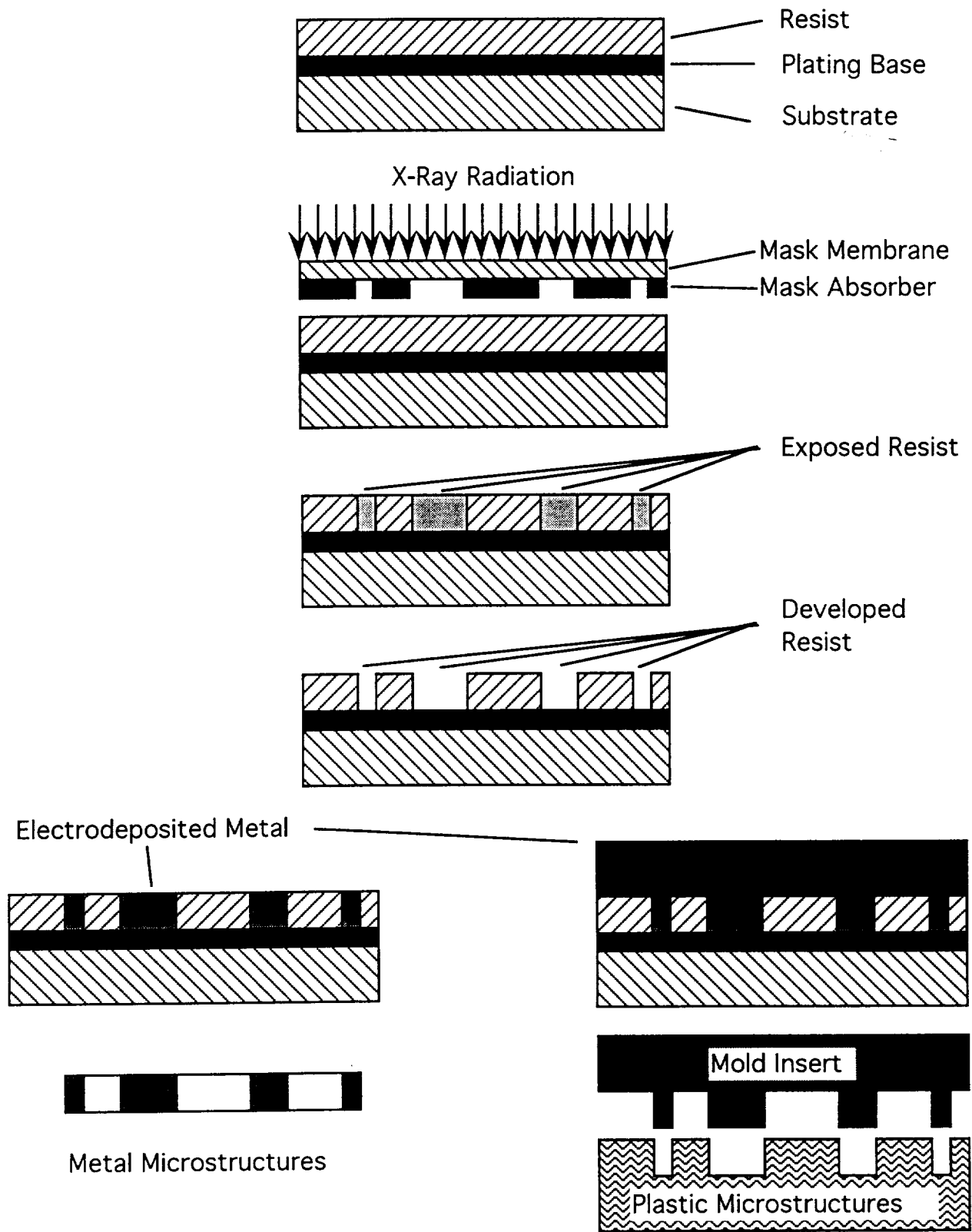


Figure 1. Steps in the basic LIGA Process.

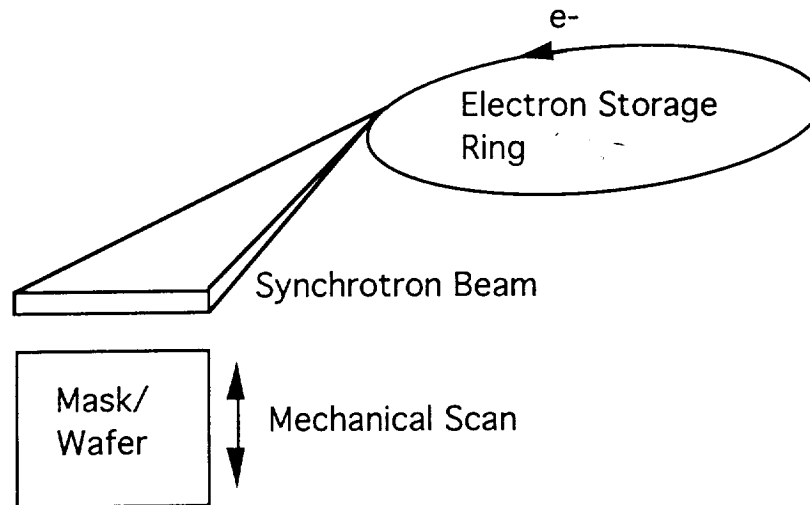


Figure 2. X-ray lithography with synchrotron radiation.

required in order to obtain more uniform exposure throughout the entire depth of a resist layer. For micromachining thicknesses up to one millimeter, the optimum wavelength for micromachining is between 0.2 and 0.5 nanometers, but shorter wavelengths have been used to pattern structures several millimeters in height (Guckel, Christenson, Earles, Klein, Zook, Ohnstein, et al., 1994).

Synchrotron sources deliver the best radiation quality for x-ray lithography (Petzold, 1988). Electrons are accelerated and injected into a ring comprised of bending magnets, which steer the electron beam. Radiation is emitted as the electron beam is turned by the magnets, as shown by the schematic in Figure 2. The emitted radiation is: (1) Broad spectrum, ranging from infrared to hard x-rays, which results in reduced Fresnel diffraction; (2) High intensity, which permits the use of low and medium sensitivity resists with adequate throughput; (3) Highly collimated, giving a high depth of focus; (4) Stable in intensity and position; and (5) Well-defined in time. All these characteristics are conducive to x-ray lithography. The emitted radiation is directed into beamlines, which may have filtering components to shape the emitted beam, but are mainly used to protect the ultra-high vacuum of the synchrotron by moving the lithography operations away from the ring.

Both positive and negative resist layers can be patterned. Most experience is with polymethylmethacrylate (PMMA) as a positive resist, although other resists are being investigated (Ehrfeld, Abraham, Ehrfeld, Lacher, & Lehr, 1994). With PMMA, the x-ray beam results in scission of long polymer chains. A highly molecular weight selective developer, in which only low molecular weight (i.e. shorter) chains are soluble, has been optimized at the IMT-KfK and is in use at most LIGA laboratories (Guckel, et al., 1990). Fabricating thick resist layers poses a significant problem. In conventional lithography resists are spun onto a substrate in thin (one micrometer or less) layers. In order to build thicker structures with this approach, several thin layers need to be spun on in succession. Without extensive annealing processes, high interfacial stresses between the layers can lead to extensive crack propagation when the exposed resist is developed. A second approach, based on a technique for casting and polymerizing thick resist layers with an optimum molecular weight distribution directly on substrates (Mohr, Ehrfeld, & Münchmeyer, 1988), has been refined at the IMT-KfK. This overcomes the problem of interfacial stresses and helps to maximize resolution of the process.

Mask technology for LIGA is more demanding than for silicon micromachining. Long exposure times are required to pattern the thick resist layers, so that technologies developed for manufacturing submicron circuitry with x-ray lithography are not directly transferable to the fabrication of micromachine elements. Mask membranes have been made from low atomic number (Z) materials including Kapton, silicon, titanium, and beryllium. In order to minimize distortion during the long exposures, which are typically hours rather than minutes long, higher strength membranes of titanium or beryllium are used (Bley, et al., 1991; Schomburg, Baving, & Bley, 1991). High contrast is obtained with high-Z absorber layers. Gold is most commonly used, with several groups looking at the viability of tungsten and other materials. In microcircuit x-ray lithography absorber layers are typically less than one micrometer thick. In comparison, a gold absorber layer must be nearly ten micrometers thick to pattern a structure 500 micrometers in height (Bley, et al., 1991). Depending on the resolution necessary for the planned structures, x-ray masks can be fabricated in different ways. The initial pattern may be generated optically or with an electron beam. That pattern is then transferred to a thick resist layer over a mask membrane using either optical or x-ray lithography. The absorber is then plated into this resist mold to create the final working mask.

Using x-ray lithography, sharp corners and vertical sidewalls have been obtained; deviations from the vertical of only $0.055 \mu\text{m}/100 \mu\text{m}$ over a height of $400 \mu\text{m}$ have been verified (Bley, et al., 1991). Resist layers up to one centimeter thick have been patterned, making the fabrication of high precision structures with lateral dimensions and thicknesses on the same order possible.

The second stage of the basic LIGA process is electrodeposition of metal into the resist mold produced using x-ray lithography (Hagmann, Ehrfeld, & Vollmer, 1989; Maner & Ehrfeld, 1988). Any metal which can be deposited either electrolytically or with electroless methods can be used, within the constraints of the materials properties of the resist mold. Gold, copper, nickel, and nickel-iron have been successfully used in structures.

Taken alone, the need for an appropriate x-ray source and x-ray masks imposes a substantial cost penalty on the LIGA process if these metal structures are the end product. The IMT-KfK group and other groups in Germany have developed techniques for maximizing the output from each mask and x-ray exposure. The exposed and developed resist can be overplated by electrodepositing a layer of metal over the entire exposed and developed mask, resulting in a mold insert. The mold insert can then be used with a plastic molding process to fabricate either plastic parts or a plastic mold for electroplating large numbers of structures. Several plastic molding processes have been tested, including reaction injection molding (Hagmann, Ehrfeld, & Vollmer, 1989), thermoplastic injection molding and thermoforming. Metal molds may also be used as forms for other materials, such as ceramics. Thus through the combination of electroplating and molding, designers using the LIGA process have access to a much broader set of engineering materials, making the process more versatile than the conventional silicon micromachining techniques.

Several extensions of the basic LIGA process have been developed. The optical properties of PMMA have been exploited in making optical couplers and a planar grating spectrograph. Structures with inclined sidewalls have been produced by tilting the angle of incidence of the x-ray beam. The roughness of the inclined sidewalls was comparable to that obtained for vertical sidewalls (40 nanometers peak-to-peak). Sacrificial layer (Burbaum, et al., 1991; Christenson, et al., 1992) and stepped structure techniques have been developed to permit fabrication of movable microcomponents. LIGA structures have been fabricated on top of integrated circuits without damaging the circuit, opening the path to integrated high aspect ratio electromechanical systems (Burbaum, et al., 1991; Christenson, et al., 1992).

Currently, development of the LIGA process is being led by three groups in Germany including the IMT-KfK. In the United States, a group at the University of Wisconsin has several years of experience with LIGA, but has not worked with plastic molding at all. Several groups have begun LIGA development including LSU/CAMD, JPL/LBL, and Louisiana Tech.

Microsystems Development at LSU

The Microsystems Engineering Team (μ SET) at LSU is focussing on development of high aspect ratio microsystems fabricated with the LIGA process or a combination of micromachining processes. The group is a collaboration between members of the Mechanical Engineering, Chemical Engineering, Chemistry, and Electrical Engineering departments at LSU and the professional staff at J. Bennett Johnston, Sr. Center for Advanced Microstructures and Devices (CAMD). Initial work on the batch fabrication of a novel toolkit for scanning probe microscopy (SPM) has led to electrodeposition in holes as small as 2 μ m in diameter and 20 μ m deep (Akkaraju, Kelly, Li, Ma, Murphy, Palshin, et al., 1994). A cooperative project with SatCon Technology for NASA Goddard is aimed at the development of micromachined actuators for micro-optical systems. Other projects include work on chemical analysis systems with the Institute for Environmental Studies at LSU, and on a unique passive ultrasound sensor for medical applications with researchers at IMT-KfK (Boerner, Horst-Meyer, Murphy, Muench, & Schomburg, 1994). The first work in the US on plastic molding of LIGA fabricated microstructures is also being carried out under an NSF-LaSER grant to establish a research cluster working on novel materials for microsystems applications.

The principal resource for microsystem development at LSU is a compact electron storage ring at CAMD. It is the first university-based synchrotron light source dedicated primarily to lithography, and currently the best source for x-ray lithography of micromechanical structures in the world. The ring is capable of 1.5 GeV, with a nominal operating energy of 1.3 GeV. Maximum current capability is 400 mA, with typical operating value of 120 mA. Figure 3 shows the current layout of the synchrotron facility. The facility opened in the fall of 1992, and the first lithography beamline, XRLC1, for microcircuit lithography was operational in the spring of 1993. Three micromachining beamlines are available: XRLM1 and XRLM2 are owned by Louisiana Tech and jointly operated by CAMD and Louisiana Tech; XRLM3, owned and operated by LSU/CAMD, came on-line in August 1994. In addition to working with μ SET, the staff at CAMD are engaged in several joint research projects including, under ARPA sponsorship, the development of the first American-built x-ray stepper and alignment system. LSU/CAMD is a partner in the Technology Reinvestment Program (TRP) Regional Micromachining Alliance and will serve as an x-ray lithography print shop for that program.

MICROMACHINED LIGHT PATH: FABRICATION PROCESS DEVELOPMENT

Gold Electrodeposition

Gold was selected as the material for the test mirror structures and light paths during the first phase of the project. An electrolytic gold electroplating solution has been purchased from Technic, Inc. based on the promised lustrous finish. Calibration of the plating parameters has led to the deposition of good quality, highly reflective gold structures.

The use of an electroless gold solution to deposit a thin layer of gold over a nickel structure, which would produce less expensive sensors, is also being investigated. An electroless gold deposition solution available from Technic deposits a thin layer of gold on a low/no phosphorous nickel base. The manufacturer suggests using an electroless nickel solution for the base. In work with electroless nickel, μ SET has successfully deposited in patterns up to 6 micrometers deep. With deeper holes, such as the mirrors, there have been problems with adhesion of the

CAMD Facility Layout

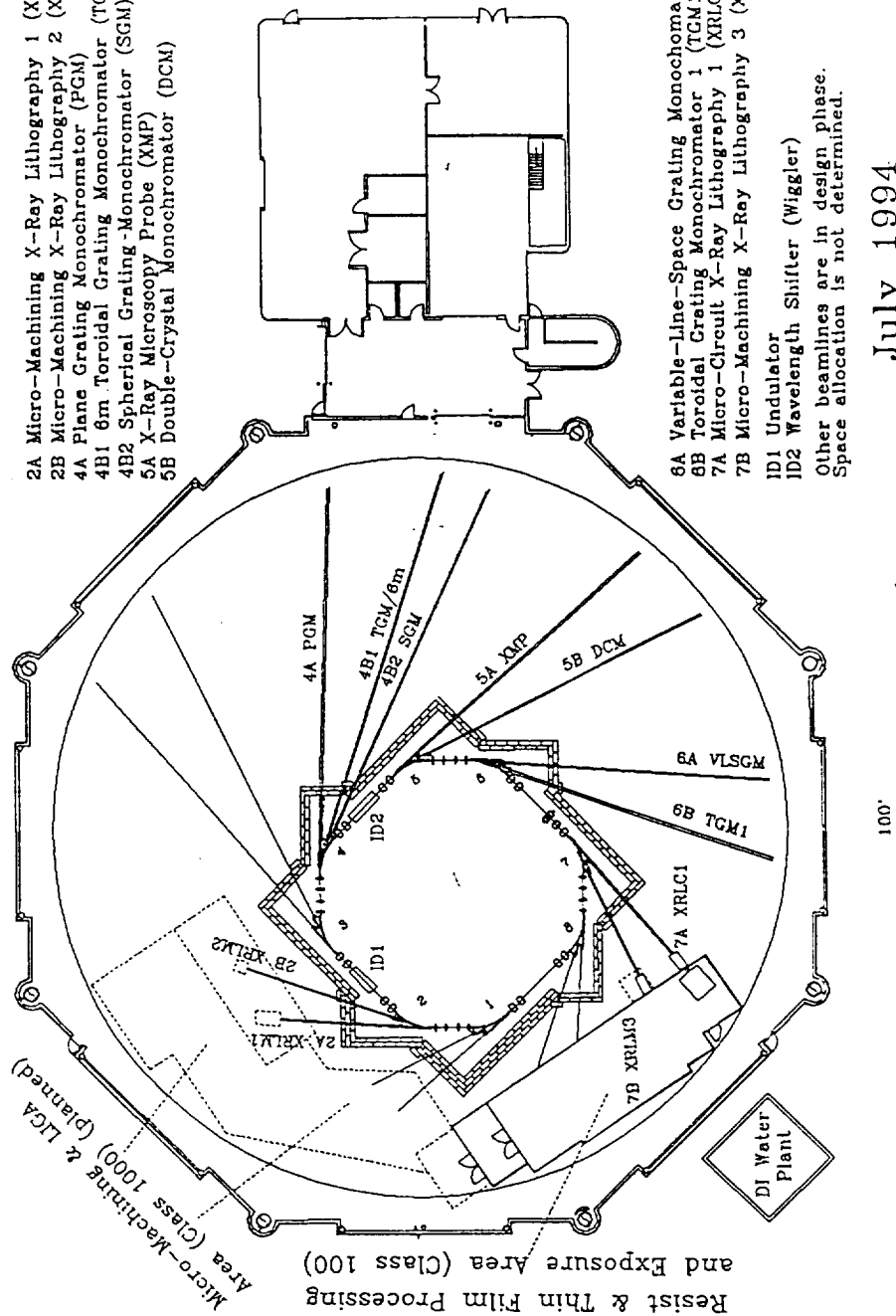
X-Ray Lithography Sector Basic Sciences Sector

Beam Lines

- 2A Micro-Machining X-Ray Lithography 1 (XRLM1)
- 2B Micro-Machining X-Ray Lithography 2 (XRLM2)
- 4A Plane Grating Monochromator (PGM)
- 4B1 6m Toroidal Grating Monochromator (TGM/6m)
- 4B2 Spherical Grating-Monochromator (SGM)
- 5A X-Ray Microscopy Probe (XMP)
- 5B Double-Crystal Monochromator (DCM)

- 6A Variable-Line-Space Grating Monochromator (VLSGM)
- 6B Toroidal Grating Monochromator 1 (TGM1)
- 7A Micro-Circuit X-Ray Lithography 1 (XRLC1)
- 7B Micro-Machining X-Ray Lithography 3 (XRLM3)

- ID1 Undulator
 - ID2 Wavelength Shifter (Wiggler)
- Other beamlines are in design phase.
Space allocation is not determined.



July 1994

Figure 3.

Current CAMD Facility. Beamlines XRLM1, XRLM2, and XRLM3 are for deep x-ray micromachining.

developed resist layer to the substrate at the temperatures required for electroless deposition. Alternative electroless nickel solutions are being investigated, but the requirement for the mirrors to be at least 100 micrometers tall appears to make this an undependable option.

In another project, μ SET has refined an electrolytic nickel plating bath which produces deposits with better than 98% nickel and only trace amounts of phosphorous. Tests have shown that gold layers, on the order of 0.6 micrometers thick, can be catalytically deposited on the electrolytic nickel from this bath. Since deep structures of electrolytic nickel have been deposited, and the deposition rate for the electrolytic nickel is much higher than for the electroless nickel, the combination of electrolytic nickel and electroless gold deposition to produce mirrors appears to be a satisfactory alternative to the direct deposition of gold mirrors. The thickness and deposition of the gold layer are highly dependent upon the pH and temperature of the plating bath. Experiments to evaluate the sensitivity of the gold layer to bath parameters are continuing.

The next step will be to evaluate the surface characteristics of the two gold surfaces using the atomic force microscope as was demonstrated in the August progress report. Breakaway structures to permit the testing of sidewall roughness have been included in the proposed mask design.

Thick Resist Layers

Formation of thick resist layers is critical to the basic LIGA process, and the fabrication of the optical bench as proposed. The initial optical bench design in the proposal called for mirror heights on the order of 100 micrometers, which requires comparable resist thicknesses. A pneumatic press and an electromechanical press are currently used by μ SET. Resists up to 250 micrometers thick have been pressed with this equipment. An alternative approach to obtaining and patterning thick resists, which uses stock Plexiglas, has been developed at CAMD and is discussed in the following section.

Some problems have been encountered with the adhesion of the thicker layers to silicon substrates with a gold plating base. This is thought to be due to flexure of the substrate under the applied resist layer and poor adhesion between the resist/plating base (gold)/silicon substrate. A series of experiments to evaluate alternatives are underway. One approach is to obtain a stiffer substrate. Copper and glass substrates are now being investigated as alternatives to the silicon. Ceramic substrates are another alternative.

Since the silicon substrate is desirable for compatibility with the light source fabrication, another alternative is to investigate the use of Ti/TiOx plating bases. Although less suitable as a plating base the titanium does form a stronger bond with the Si/SiOx surface of the substrate. Vendors for silicon substrates with titanium plating bases are being sought. Consultation with the LIGA group at KfK in Germany, confirmed this experience with the silicon substrates.

Alternative Fabrication Process/Design

A novel sacrificial or transfer mask technique has been developed and patented by CAMD researchers (Vladimirsky, Vladimirsky, Saile, Morris, Klopff, Murphy, et al., 1995). It can be used to fabricate mirror structures inexpensively. Using an optical photomask, a thin layer of optical resist on top of the is patterned directly on plexiglas. The pattern is developed and gold is electrodeposited. When the remaining photoresist is removed, the x-ray absorber for the exposure has been deposited directly on top of the substrate/resist, avoiding most of the expense and difficulty of purchasing or making an x-ray mask. Exposure to x-rays produces deep

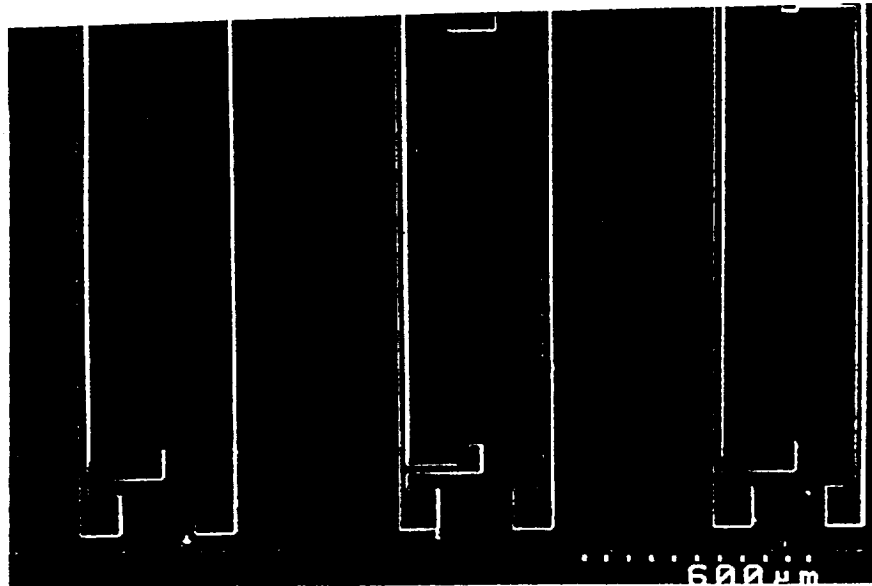


Figure 4. Top view of gold plated plexiglas structures suitable for use as inexpensive mirrors. The parallel structures are similar to one of the proposed light path designs.

structures in the plexiglas. When coated with evaporated gold, these structures are suitable alternatives to the proposed mirrors.

The process has been used to fabricate deep structures, on the order of 250 micrometers. Figure 4 shows a top view of several structures, in an arrangement similar to one of the proposed light paths. Views showing the sidewall finish and reflectivity of the surface are shown in Figures 5 and 6.

This process could be applied to the fabrication of the light paths by bonding the resist to the substrate and fabricating the light path. Compatibility of the bonding agent and the light source will have to be investigated in detail if this approach is taken.

MICROMACHINED LIGHT PATH: MASK LAYOUT

A mask pattern containing test structures for surface roughness evaluation and light paths based on the initial concept is complete and shown in Figure 7 (with light rays shown on the light paths). The layout contains three model light paths in the upper portion: (1) flat mirrors in a spiral arrangement (as in the proposal), (2) flat mirrors in a parallel arrangement, and (3) parabolic mirrors in a parallel arrangement. Note that the parabolic mirrors would focus the beam in the plane of the substrate, but not vertically. The layout also contains a set of test structures, the most important being the isolated mirrors which can be separated from the substrate for AFM scanning of the sidewall surface roughness (see the initial project report).

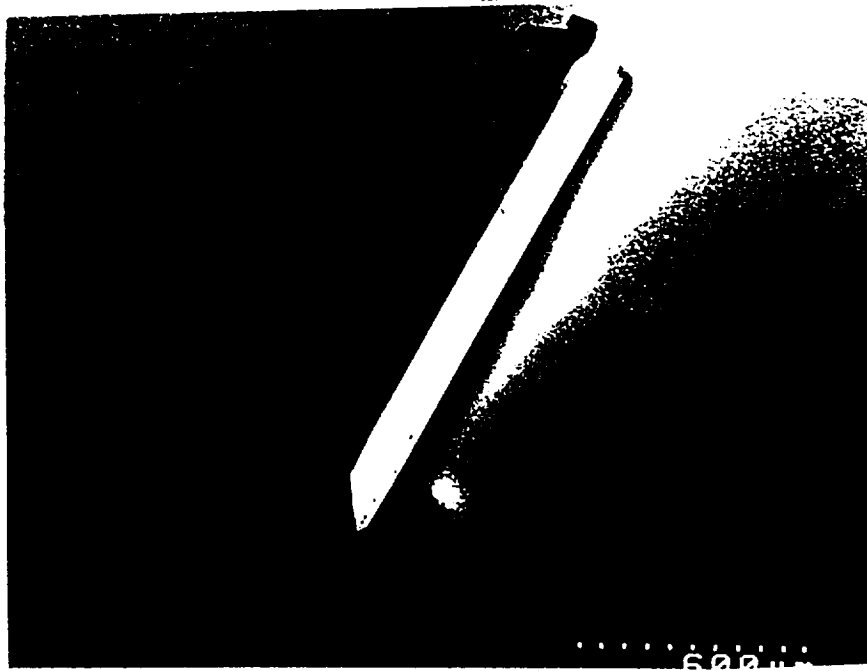


Figure 5. View of a single gold plated plexiglas structure suitable for use as inexpensive mirrors. The structure is on the order of 250 micrometers high and over a millimeter in length.

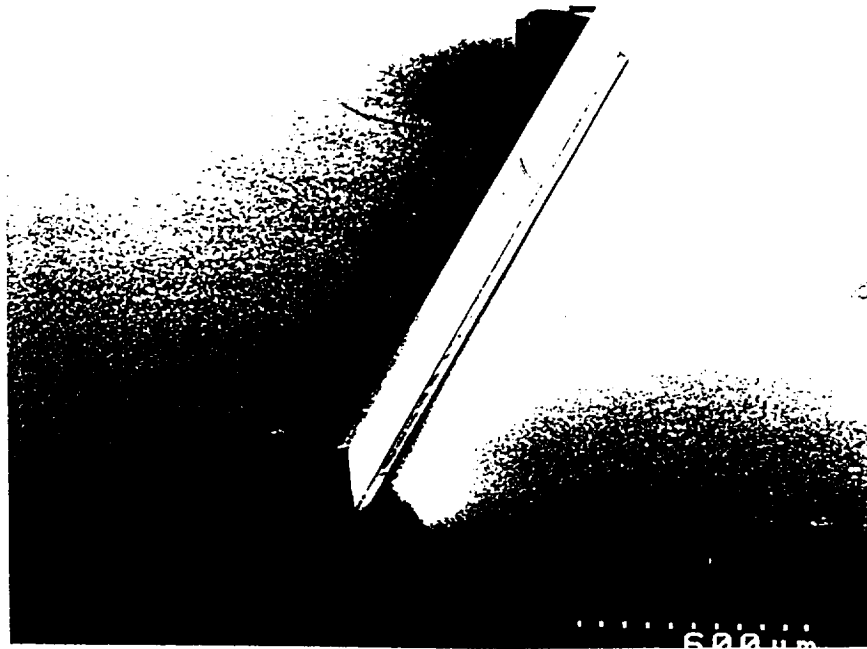


Figure 6. View of a single gold plated plexiglas structure suitable for use as inexpensive mirrors. Notice the surface finish of the sidewall.

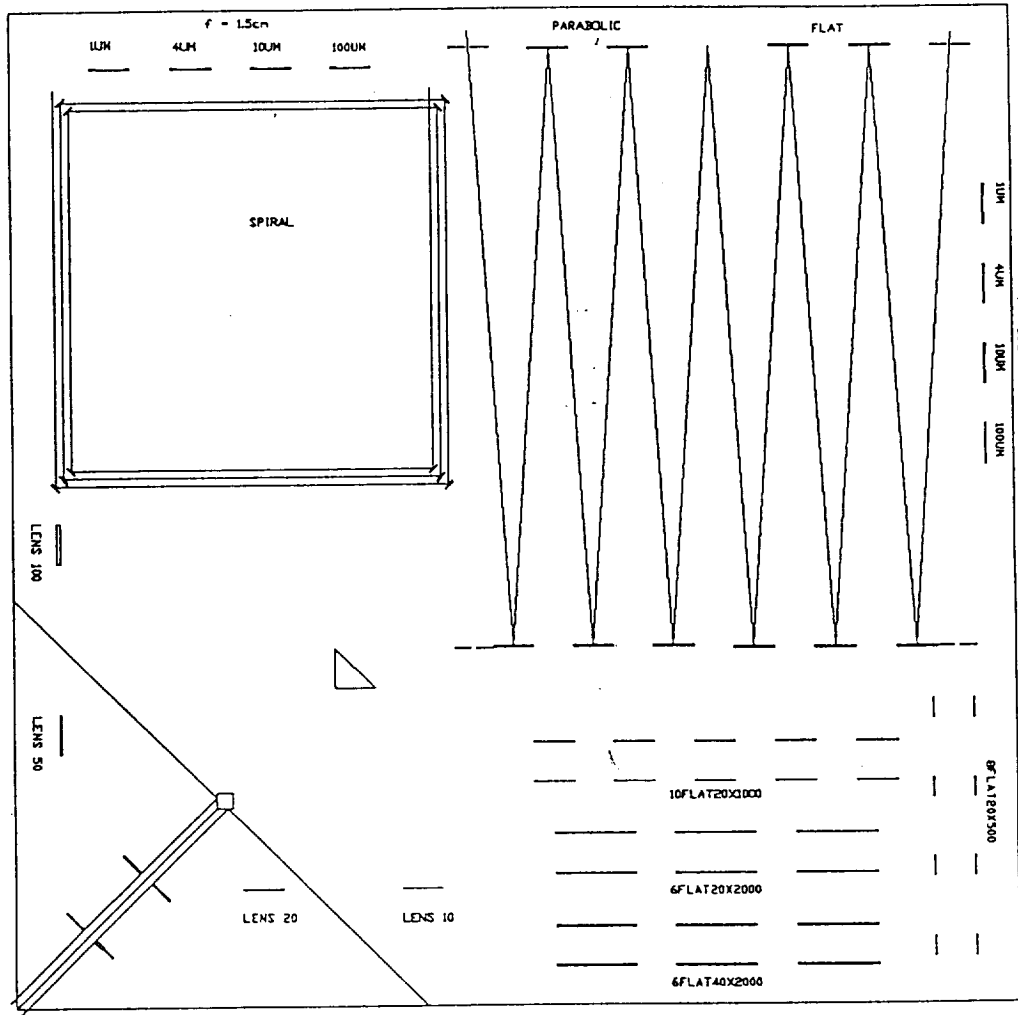


Figure 7. Mask layout for CO₂ sensor light paths and test structures.

Sidewall roughness is expected to be a function of the lithography process and plating parameters, while top surface roughness is primarily a function of the plating parameters.

Two mask producers (DuPont, IBM) have been contacted for possible quotes on a mask.

MICROMACHINED LIGHT PATH: ANALYSIS

Light Path Limitations: Surface Roughness

Surface roughness effects were analyzed in the prior report. Surface roughness will lead to scattering of the incident beam. In order to have an accurate sensor, the level of surface roughness losses must be characterized. The atomic force microscope (AFM) will be a suitable tool for this evaluation, when structures are available.

Scattering theory was used to relate the spectral reflectance of a theoretical mirror surface to the surface roughness. The ratio of specular reflectance to total reflectance is given by (Bennett & Mattson, 1989):

$$\frac{R_s}{R_o} = e^{-(4\pi\delta \cos \theta_o/\lambda)^2}$$

Assuming the total reflectance, R_o , for a super-polished gold surface is approximately 0.98, the theoretical spectral reflectance of gold mirrors was calculated as shown in Figure 8. The angle of incidence is measured from the mirror surface. The reflectance after five reflections is shown in Figure 9. Note that the number of reflections and the angle of incidence strongly effect the spectral reflectance.

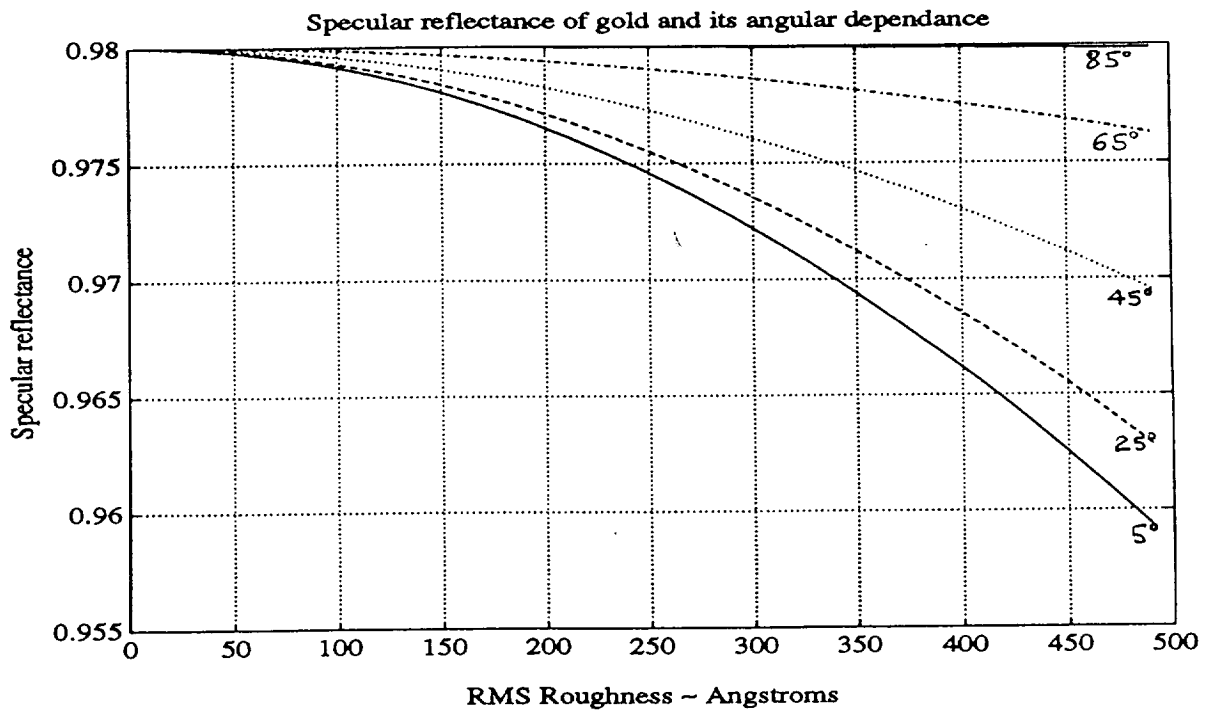


Figure 8. Spectral reflectance of gold as a function of rms surface roughness and angle of incidence.

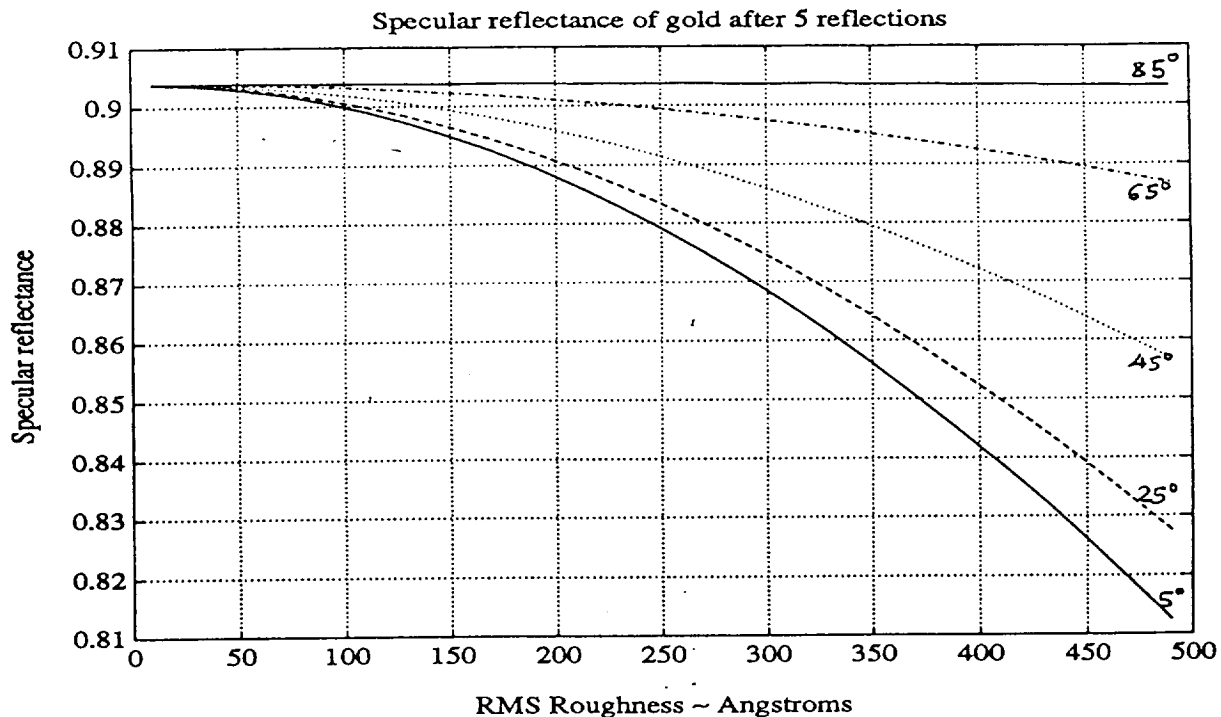


Figure 9. Spectral reflectance of gold after five reflections as a function of rms surface roughness and angle of incidence.

Light Path Limitations: Diffraction/Divergence

A laser light source would present the best case for beam divergence due to diffraction. The divergence of a laser beam due to diffraction was evaluated for several conditions in order to establish the bounds on fabrication, mirror geometry, and source geometry.

For a laser with a Gaussian intensity profile across the beam, the variation of the beam spot size is given by (Koegelnik, 1979):

$$w_z^2(z) = w_o^2 \left[1 + \left(\frac{\lambda z}{\pi w_o^2} \right)^2 \right]$$

where the initial spot radius is w_o , the spot radius is w_z , the distance traveled by the beam is z , and the wavelength, λ . The optimum wavelength for CO₂ detection, which is projected for use in the final sensor, is 4.2 micrometers. A second CO₂ absorption peak occurs at 10.6 micrometers, but water vapor absorption is also high at this wavelength. No laser with the optimum 4.2 μm wavelength is readily available at either LSU or NASA, but a 10.6 μm laser with approximately a 50 micrometer beam spot radius could be available for light path evaluation at LSU.

Initial beam divergence calculations were made for the proposed experimental conditions: a laser source with a wavelength of 10.6 μm and an initial spot radius of 50 μm . Mirrors were assumed to be 1000 micrometers wide and 100 micrometers high, consistent with the mask

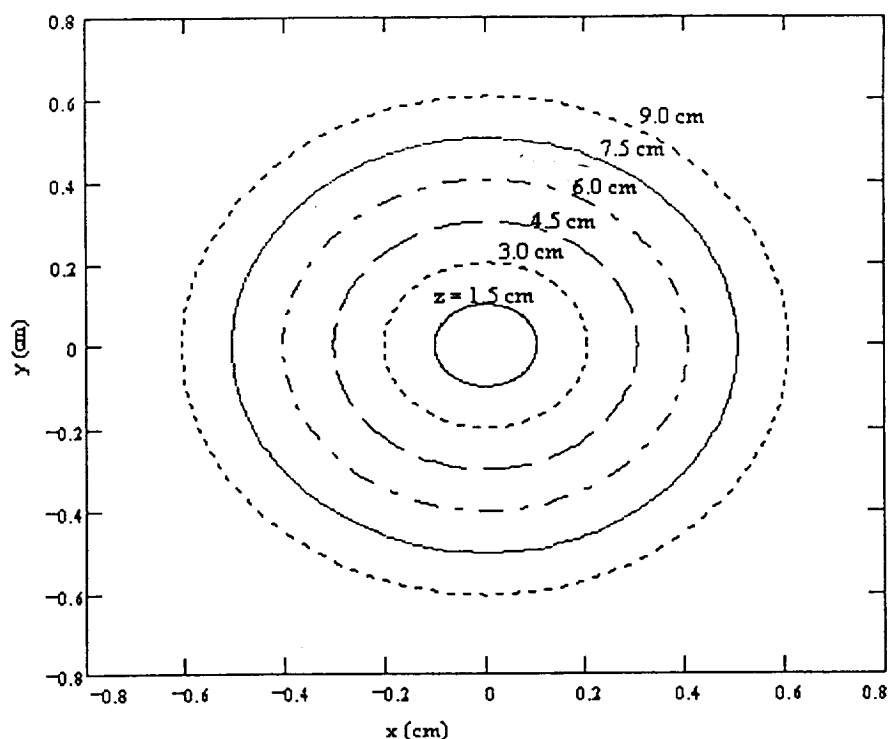


Figure 10. Divergence of a 100 μm diameter, 10.6 μm wavelength light beam at increments of 1.5 cm. of path length. At 9 cm. the beam has diverged to a radius of 6 mm. Total path length for the prototype sensor is projected to be 10 cm.

layout and proposal. The results of these calculations are shown in Figure 10. The first plot shows the cross-section of the beam at 1.5 centimeter increments of the light path length. At 1.5 centimeters, the distance to the first mirror in the mask layout, the beam radius has expanded from an initial radius of 50 μm to a radius of approximately 1000 μm . After 9 centimeters (for ppm resolution the actual path length must be greater than 10 centimeters), the radius is 0.60 centimeters. With the assumed mirror dimensions, only a small percentage of the photons would impinge on the first mirror. If that percentage is taken to be proportional to ratio of the area of the mirror to the area of the beam, the loss at the first at the first mirror would be on the order of ninety-seven percent. Transmission of the light to the remaining mirrors in the light path would be complicated by the asymmetry in the mirror geometry. The mirror dimensions needed to avoid these conditions could not be fabricated using the current x-ray lithography resources at CAMD. The bound on mirror height with the micromachining beamline is approximately 1000 micrometers.

Since the actual sensor light source would have a wavelength of 4.2 μm , the calculations were repeated assuming the same initial beam spot radius and mirror dimensions were the same but the source wavelength was consistent with the final design. Figure 11 shows the result which, although improved with a beam radius at 9 centimeters of 0.24 centimeters, is still beyond the current microfabrication capacity.

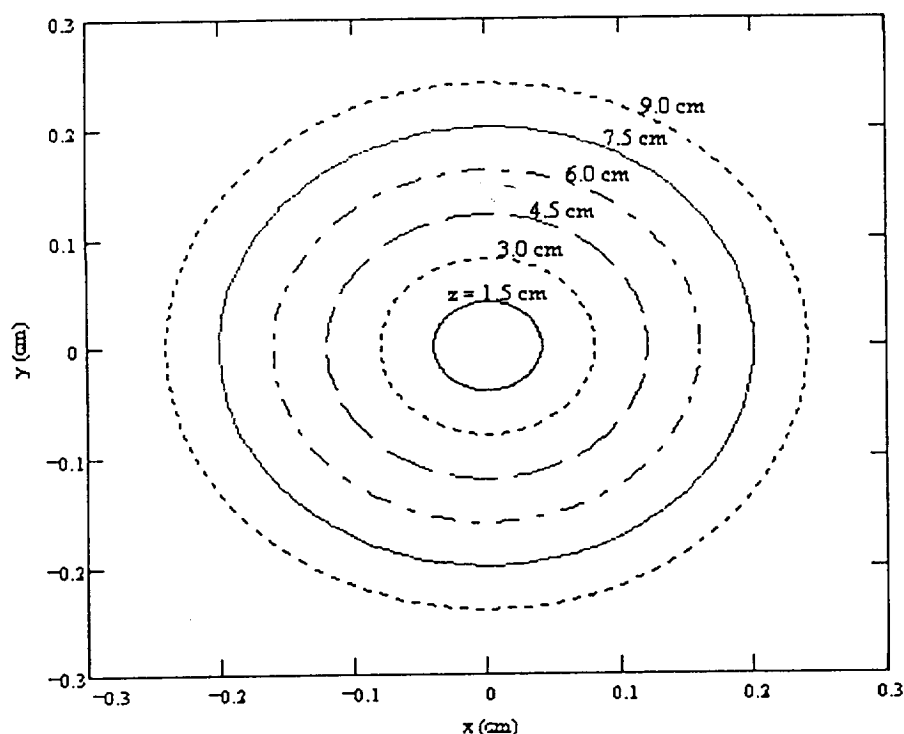


Figure 11. Divergence of a 100 μm diameter, 4.2 μm wavelength light beam at increments of 1.5 cm. of path length. At 9 cm. the beam has diverged to a radius of 2.4 mm. Total path length for the prototype sensor is projected to be 10 cm.

The infrared wavelengths for the sensor and the concept evaluation are fixed, but the mirror and beam spot radius are variables in the sensor design. The upper bound placed on the mirror height by the fabrication process is 1000 micrometers. The dimensions of the source beam have not been fixed. The calculations were repeated with the source initial beam radius as a variable to determine if there were any combinations of source and mirror dimensions which could be microfabricated and produce a sensor design consistent with the proposed concept. The variation in the beam spot radius of a 10.6 μm source over a distance of 1.5 centimeters is shown in Figure 12. For initial radii greater than approximately 600 micrometers there is no significant divergence of the beam. For beam radii between 400 micrometers and 600 micrometers there is only slight expansion.

A beam expansion coefficient, ϵ_i , can be defined as the ratio of the beam spot radius at a given distance to the initial radius:

$$\epsilon_i = \frac{W_z}{W_0}$$

For an initial spot radius of 50 μm , the expansion coefficient is 20.3, but for an initial radius of 300 μm the coefficient is reduced to 1.15 (Figure 13). A concept evaluation structure could be fabricated with mirrors on the order of 1000 μm by 1000 μm for use with sources with initial beam radii between 300 μm and 500 μm and eliminate losses due to beam divergence.

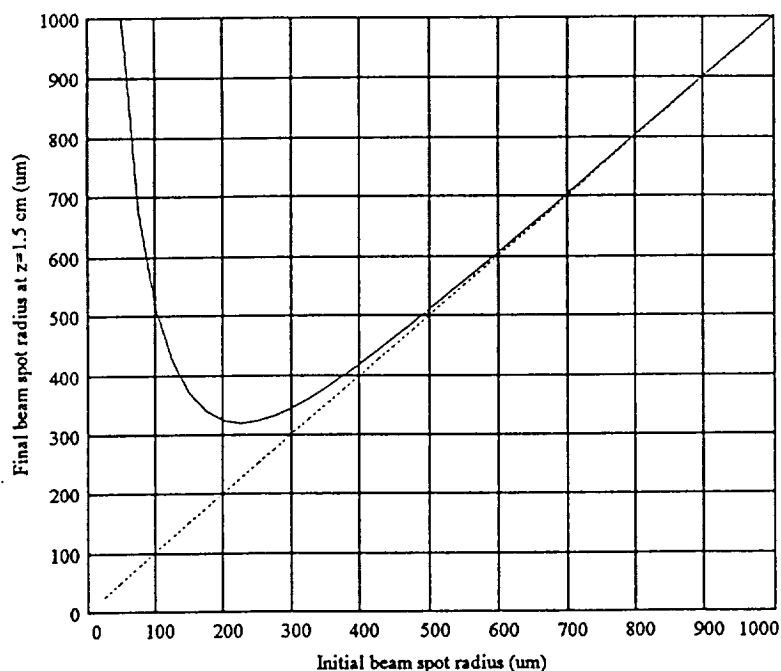


Figure 12. Beam spot radius at 1.5 centimeters as a function of the initial spot radius for a 10.6 μm laser source.

Evaluation of beam expansion and beam expansion coefficient for the actual sensor wavelength of 4.2 μm produces similar results with the expected improvement. Figure 14 and Figure 15 show that the beam expansion coefficient is reduced to 1.025 for a 300 μm initial beam radius, so that mirrors greater than 600 μm high should eliminate diffraction as a significant issue in the final light path design.

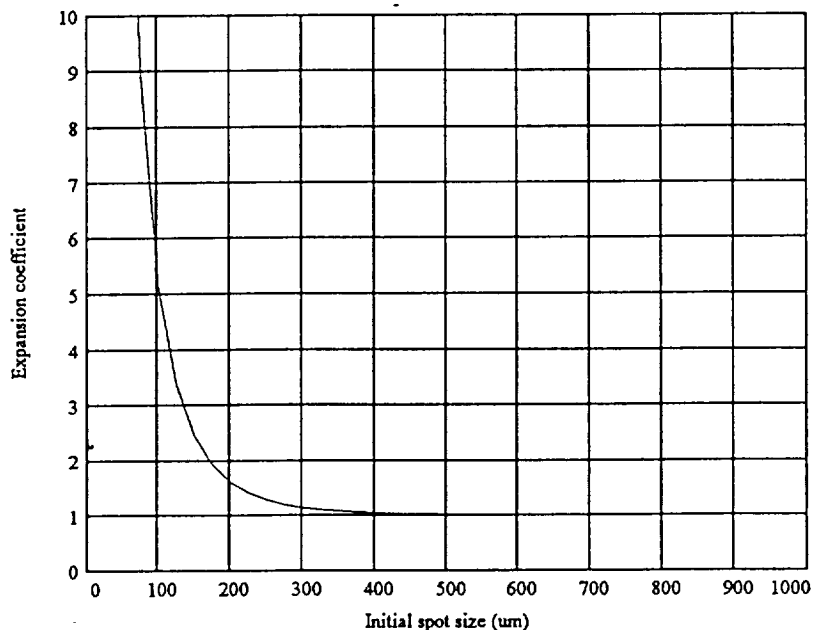


Figure 13. Beam expansion coefficient at 1.5 centimeters as a function of initial spot radius for a 10.6 μm laser source.

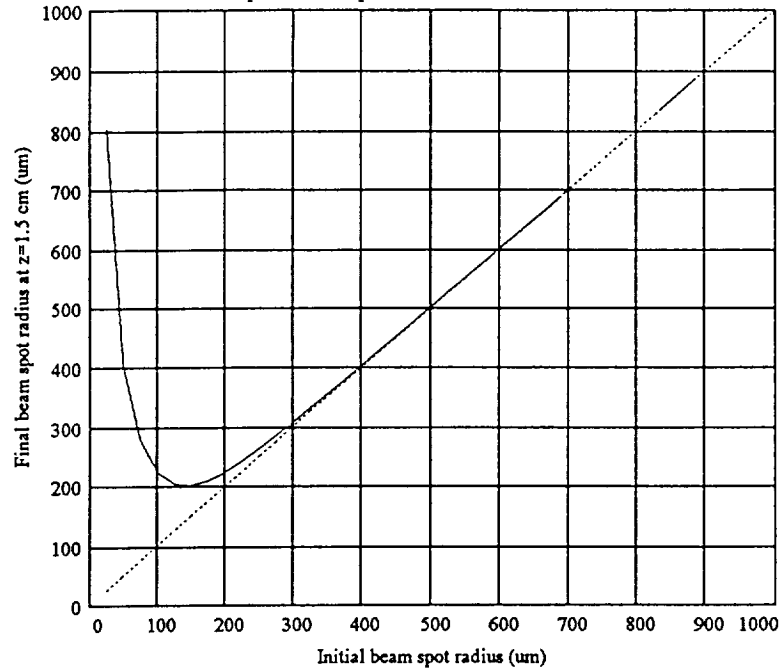


Figure 14. Beam spot radius at 1.5 centimeters as a function of the initial spot radius for a 4.2 μm laser source.

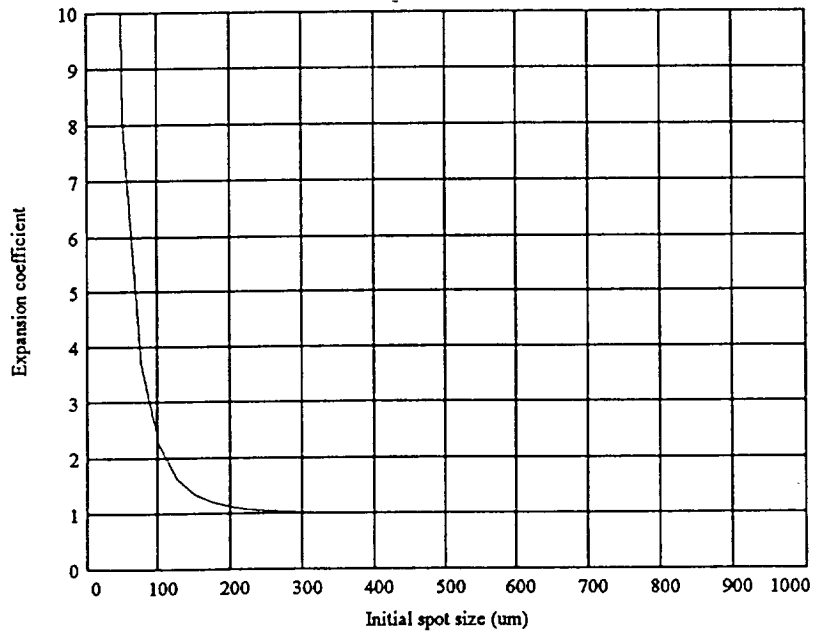


Figure 15. Beam expansion coefficient at 1.5 centimeters as a function of initial spot radius for a 4.2 μm laser source.

SUMMARY

Significant progress has been made toward all of the goals for the first phase of the project short of actual fabrication of a light path. Two alternative approaches to fabricating gold mirrors using the basic LIGA process were developed, one using electroplated solid gold mirrors and the second using gold plated over a nickel base. A new method of fabrication, the transfer mask process, was developed and demonstrated. It can be used to either create mirror structures of PMMA coated with evaporated gold or to in the x-ray lithography step necessary to fabricate mirrors using the first two approaches.

Analysis of the projected surface roughness and beam divergence effects was completed. With gold surface with low surface roughness scattering losses are expected to be insignificant. Beam divergence due to diffraction will require a modification of the original design, but should be eliminated by fabricating mirrors 1000 μm in height by 1000 μm in width and using a source with an initial beam radius greater than 300 μm . This may eliminate any need for focussing optics.

Since the modified design does not affect the mask layout, ordering of the mask and fabrication of the test structures can begin immediately at the start of Phase I.

BIBLIOGRAPHY

Akkaraju, S., Kelly, K., Li, B., Ma, E., Murphy, M., Palshin, V., Wang, W., Madou, M., Vladimirov, O., & Vladimirov, Y. (1994). Tips for scanning probe microscopy produced with LIGA. In P. J. Hesketh, J. N. Zemel, & H. G. Hughes (Ed.), Symposium on Microstructures and Microfabricated Systems, 185th Meeting of the Electrochemical Society, 94-14 (pp. 188-195). San Francisco, CA: The Electrochemical Society.

Bennett, J. M., & Mattson, L. (1989). Introduction to Surface Roughness and Scattering. Washington, D.C.: Optical Society of America.

Bley, P., Menz, W., Bacher, W., Feit, K., Harmening, M., Hein, H., Mohr, J., Schomburg, W. K., & Stark, W. (1991). Application of the LIGA process in fabrication of three-dimensional mechanical microstructures. In S. Namba & T. Tsurushima (Ed.), MicroProcess 91, 1991 International MicroProcess Conference, (pp. 384-389). Kanazawa, Japan:

Boerner, M. W., Horst-Meyer, S. z., Murphy, M. C., Muench, H.-J., & Schomburg, W. K. (1994). Contactless ultrasonic measurements with micromembranes. In Eurosensors VIII, .

Burbaum, C., Mohr, J., Bley, P., & Menz, W. (1991). Fabrication of capacitive acceleration sensors by the LIGA technique. Sensors and Actuators A, 25-27(1/3), 559-563.

Christenson, T. R., Guckel, H., Skrobis, K. J., & Jung, T. S. (1992). Preliminary results for a planar microdynamometer. In IEEE Solid-State Sensor and Actuator Workshop, (pp. 6-9). Hilton Head, SC: IEEE.

Ehrfeld, W., Abraham, M., Ehrfeld, U., Lacher, M., & Lehr, H. (1994). Materials for LIGA products. In IEEE Workshop on Micro Electro Mechanical Systems, (pp. 86-90). Oiso, Japan: IEEE Press.

Guckel, H., Christenson, T. R., Earles, T., Klein, J., Zook, J. D., Ohnstein, T., & Karnowski, M. (1994). Laterally driven electromagnetic actuators. In D. S. Eddy (Ed.), Solid-State Sensor and Actuator Workshop, (pp. 49-52). Hilton Head, SC: Transducers Research Foundation, Inc.

Guckel, H., Christenson, T. R., Skrobis, K. J., Denton, D. D., Choi, B., Lovell, E. G., Lee, J. W., Bajikar, S. S., & Chapman, T. W. (1990). Deep x-ray and uv lithographies for micromechanics. In D. S. Eddy (Ed.), IEEE Solid-State Sensor and Actuator Workshop, 1 (pp. 118-122). Hilton Head, SC, USA: IEEE.

Guckel, H., Skrobis, K. J., Christenson, T. R., Klein, J., Han, S., Choi, B., & Lovell, E. G. (1991). Fabrication of assembled micromechanical components via deep x-ray lithography. In IEEE Workshop on Micro Electro Mechanical Systems, (pp. 74-79). Nara, Japan: IEEE Press.

Hagmann, P., Ehrfeld, W., & Vollmer, H. (1989). Fabrication of microstructures with extreme structural heights by reaction injection molding. Makromolekulare Chemie - Macromolecular Symposia, 24, 241-251.

Koegelnik, H. (1979). Propagation of Laser Beams. In R. R. Shannon & W. C. Wyant (Eds.), Applied Optical Engineering (pp. 157-190). New York: Academic Press.

Maner, A., & Ehrfeld, W. (1988). Electroforming techniques in the LIGA process for the production of microdevices. In InterFinish 88, 12th World Congress on Metal Finishing, 2 (pp. 577-586). Paris, France:

Menz, W., Bacher, W., Harmening, M., & Michel, A. (1991). The LIGA technique -- a novel concept for microstructures and the combination of Si-technologies by injection molding. In IEEE Workshop on Micro Electro Mechanical Systems, (pp. 69-73). Nara, Japan: IEEE Press.

Mohr, J., Ehrfeld, W., & Münchmeyer, D. (1988). Requirements on resist layers in deep-etch synchrotron radiation lithography. Journal of Vacuum Science Technology B, 6(6), 2264-2267.

Petzold, H.-C. (1988). X-Ray Lithography. In Applications of Synchrotron Radiation London, UK: Gordon and Breach Science Publishers Ltd.

Schomburg, W. K., Baving, H. J., & Bley, P. (1991). Ti- and Be- x-ray masks with alignment windows for the LIGA process. Microelectronic Engineering, 13, 323-326.

Vladimirsky, Y., Vladimirsky, O., Saile, V., Morris, K., Klopf, M., Murphy, M. C., & Desta, Y. M. (1995). X-ray and uv transfer mask for high aspect ratio lithography. In International Conference on Solid-State Sensors and Actuators (Transducers '95), . Stockholm, Sweden: